Honda Research Institute EU
Honda Research Institute Europe GmbH
https://www.honda-ri.de/

Working area mapping with an autonomous lawn mower

Nils Einecke, Keiji Muro, Jörg Deigmöller, Mathias Franzius

2017

Preprint:

This is an accepted article published in Field and Service Robotics. The final authenticated version is available online at:
https://doi.org/10.1007/978-3-319-67361-5_23

Boundary Wire Mapping on Autonomous Lawn Mowers

Nils Einecke and Jörg Deigmöller and Keiji Muro and Mathias Franzius

Abstract Currently, the service robot market mainly consists of floor cleaning and lawn mowing robots. While some cleaning robots already feature SLAM technology for the constrained indoor application, autonomous lawn mowers typically use an electric wire for boundary definition and homing towards to charging station. An intermediate step towards SLAM for mowers is mapping of the boundary wire. In this work, we analyze three types of approaches for estimating the boundary of the working area of an autonomous mower: GNSS, visual odometry, and wheel-yaw odometry. We extended the latter with orientation loop closure, which gives the best overall result in estimating the metric shape of the boundary.

1 Introduction

Autonomous lawn mowers are on the verge of a major market in the lawn and garden segment. The segment is still small with an installation volume of 103k units in 2015 [8]. However, the market for autonomous mowers is growing quickly (25% in 2015 [8]), mostly because the robot mowers increase their owner's leisure time, while maintaining good cutting results.

Currently, autonomous vacuum cleaning robots [3, 6, 16] and autonomous lawn mowers [9, 3] are the most promising entry points for robots at home. While high-end research robots for household tasks are typically too expensive and not robust enough for 24/7 application, autonomous vacuum cleaning and autonomous lawn mowers have become a robust and stable platform. For vacuum cleaners, there is

Nils Einecke, Mathias Franzius, Joerg Deigmoeller
Honda Research Institute Europe GmbH, Carl-Legien-Strasse 30, 63073 Offenbach/Main, Germany, e-mail: firstname.lastname@honda-ri.de

Keiji Muro
Honda R&D Co., Ltd. Power Products R&D Center, 3-15-1 Senzui, Asaka-shi, Saitama, 351-0024 Japan, e-mail: keiji.muro@h.rd.honda.co.jp

an active research especially for vision SLAM [10, 11, 12]. However, autonomous lawn mowers still lack intelligent functions known from state of the art research like mapping, object recognition, obstacle avoidance, localization, dynamic path planning or speech recognition.

Almost all autonomous lawn mowers use a boundary wire emitting an electromagnetic signal for limiting the working area and for homing to the charging station. Typically, robotic lawn mowers move randomly within the boundary wire. Such a system is simple and reliable and does not require localization during operation. However, finding the charging station, for example, requires searching and following the wire. Direct navigation to the charging station would obviously be more efficient.

In this work, we compare different sensors and methods for estimating a boundary wire map (see Fig. 2), which is an intermediate step towards localization. Given a map as produced by our approach, and measurement of wire signals, localization is a much easier problem than full SLAM, e.g. using Particle Filtering [18]. Localization is the basis for more intelligent behavior of the robot mower, like direct start (move from the base station directly to a user defined position), direct home (directly move to the base station without following the wire), or mowed area bookkeeping (mower keeps track of mowing time in certain zones like front yard).

2 Related Work

Publications specifically on autonomous lawn mowers are scarce. In [20, 21] an omni-directional position estimation system for an autonomous lawn mower was introduced. The authors used an off-the-shelf robotic mower and extended it with an omni-camera and an additional compute unit. In their latest work [21] the equipment was nicely integrated in a near-product fashion. Unfortunately, the outdoor results were not compared with state of the art approaches. Another example for localization on a lawn mower uses odometry, a gyroscope, and an additional RFID system [13]. While detection of the RFID tags can compensate for drift, this system requires additional infrastructure in the garden.

Besides the few mower-specific work there is a large base of research on outdoor navigation. In the automotive domain, the online KITTI benchmark [7] has become a standard tool for the comparison of state of the art visual odometry (VO) methods. The different approaches are evaluated against ground truth trajectories generated by a fusion of GPS and IMU data. In contrast to the KITTI VO benchmark, our focus is on the robot navigation in garden environments which have a different characteristic.

Odometry accumulates drift, which can be corrected by external measurements, such as visual outdoor localization. The robustness of visual localization depends on invariance against appearance changes on different time scales (e.g. lighting, weather, seasons). Popular local descriptors like SIFT and SURF are prone to fail in these conditions [19]. However, recently there has been increased interest to develop long-term robustness for visual localization (e.g., [17, 14]).

In this publication, we concentrate specifically on garden environments, which are typically relatively small and with poor GNSS reception. Our test gardens were equipped with border wires that allowed method comparisons under precise path repetitions. While camera-based systems have high potentials, we will show that a low-cost wheel odometry system can be competitive or better in these specific settings.

3 Approach

As explained above our target is to accurately estimate the garden layout. Our idea is to let the autonomous mower follow the wire while recording sensor data.

3.1 GNSS

Global navigation satellite systems (GNSS) like GPS can be an easy out-of-the-box solution for many localization problems. However, GNSS localization quality strongly depends on the visibility of satellites. At least four satellites must be visible simultaneously in order to compute the receiver's location. Localization quality also depends on the angular distribution of satellites in the sky, and it can strongly decrease if signals are not received directly but as reflections from nearby objects. Thus, the operating conditions for GNSS in a typical garden environment can be extremely bad, given that trees and buildings often shadow or reflect the direct line-of-sight. We considered three improvements for the accuracy: RTK, an additional base station for differential mode, and IMU integration.

In April 2016 we commissioned a study from the institute of Physical and Satellite Geodesy at Technical University Darmstadt for one of our test gardens to compare a high-end reference GNSS system with a low-cost system. The high-end system was based on two Novatel ProPak-V3 and the cheap system on one u-blox ANTARIS AEK-4T. Average accuracy of the reference system in this garden was just below $0.5m$, while the u-blox ANTARIS AEK-4T often yielded position errors more than 2 magnitudes higher. Only after the end of the study in April 2016, the new cm-precision low-cost differential RTK system u-blox C94M8P became available. We found that this system outperformed the reference system of the earlier study. Hence, we only show results for the new u-blox system.

3.2 Wheel Odometry

In general, the movement of an autonomous lawn mower is described by differential drive kinematics [5]. This means autonomous lawn mowers typically have two

independent drive wheels located on one axis. Using the principle of instantaneous center of curvature the movement of the mower system can be computed from just the velocities of the two wheels:

$$\begin{bmatrix} \Delta x \\ \Delta y \\ \Delta \theta \end{bmatrix} = \begin{bmatrix} cos(\omega\Delta t) & -sin(\omega\Delta t) & 0 \\ sin(\omega\Delta t) & cos(\omega\Delta t) & 0 \\ 0 & 0 & 1 \end{bmatrix} \begin{bmatrix} Rsin(\theta) \\ -Rcos(\theta) \\ 0 \end{bmatrix} + \begin{bmatrix} Rsin(\theta) \\ Rcos(\theta) \\ \omega\Delta t \end{bmatrix}, \quad (1)$$

where

$$R = \frac{l}{2}\frac{v_r + v_l}{v_r - v_l} \quad (2)$$

$$\omega = \frac{v_r - v_l}{l}. \quad (3)$$

In these equations v_l and v_r are the left and right wheel velocity, respectively. The distance along the axis between the two wheels is l. The actual wheel velocities are calculated from the wheel turning rates.

It is well known that the wheel odometry heavily suffers from wheel slip which is in particular true for autonomous lawn mowers as grass tends to be slippery when wet. Hence, in addition to the wheel rate, we also record the yaw sensor data of the autonomous lawn mower. Since the orientation estimation in the differential drive equation (1) is independent of the position estimation, the computed orientation changes $\Delta\theta$ can be replaced by measured orientation changes $\Delta\theta_{yaw}$. In the remainder, we will refer to this as yaw sensor enhanced wheel odometry (yWO).

Unfortunately, the standard differential drive kinematics are defined for 2D movements. However, not all gardens are flat. Thus, we additionally record data from the mower's accelerometer. Please note that in Europe autonomous mowers require to have a tilt sensor in order to automatically switch off the mowing blades in case of a turn over. Typically, this tilt sensor is an accelerometer. Using this data it is possible to rotate the 2D movement computed by means of the differential drive equation (1) in 3D such that actually 3D movements can be estimated.

3.3 Visual Odometry

Simply put, visual odometry (VO) is odometry estimation using cameras. The basic idea is to use the apparent image motion in order to derive the movement of the camera. In the single camera case the estimation struggles with a scale problem, i.e. the algorithms have to estimate metric distances by clever assumptions and integration over time. Using stereo cameras, this problem is directly solved by available depth information. We decided to concentrate on VO based on stereo cameras as the correct metrics are very crucial for our boundary wire estimation target.

We use two different VO approaches in this work: the stereo version of ORB-SLAM [15] and NOTF [4]. ORB-SLAM is a full blown algorithm for simultaneous

localization and mapping. VO is just one piece in this complex algorithm. ORB-SLAM also encompasses a key-frame based pose graph construction, local and global refinements using bundle adjustment, 3D map building and place recognition. For our needs mainly the estimated camera path is interesting, however, the other parts of the algorithm indirectly contribute to this path estimation thereby potentially improving it.

In contrast to ORB-SLAM, NOTF is a pure VO algorithm. It does neither involve any kind of temporal filtering like bundle adjustment nor does it build up a map of the environment. Essentially, NOTF is a simple frame by frame estimation framework. Nevertheless, it ranks very high in the KITTI benchmark [7]. Due to its concentration on pure VO and simple nature but high performance on KITTI we decided to include NOTF in our comparison.

3.4 Weighted Loop Closure

Position estimated by wheel odometry or visual odometry both drift over time due to error accumulation in the single movement estimation steps. Full blown SLAM algorithms like ORB-SLAM tackle this problem by relocalization using features stored along with the map data. Once a position is detected as being revisited, a loop closure is done. The idea of loop closing is to realign the position estimates between the two visits of the same point such that the estimated position of the two visits is the same. This leads to a strong improvement of the position estimation for visual SLAM methods compared to pure VO methods. For wheel odometry this is more difficult as the detection of revisiting the same position is very difficult without additional data as from a camera.

The situation in our scenario of boundary wire layout estimation is more favorable. Since the autonomous lawn mower starts and ends in the base station the start and end point are known to be the same. This makes it possible to also compute a loop closure for the wheel odometry.

The naïve approach for loop closing (LC) is to distribute the position error equally to all n estimated positions $p = (x, y)$ within the loop:

$$p_{err} = p_{end} - p_{start} \tag{4}$$

$$\Delta p_i^{corr} = \Delta p_i - \frac{1}{n} p_{err} \tag{5}$$

In our experiments, we found this correction to work but having some issues especially at points where the position of the mower does not change much, e.g. during turning or standing at the base station. Hence, we propose a weighted error distribution based on the movement distance:

$$d_i = |p_i - p_{i+1}|^2 \tag{6}$$

$$d_{all} = \sum_i d_i \tag{7}$$

$$\Delta p_i^{corr} = \Delta p_i - \frac{d_i}{d_{all}} p_{err} \tag{8}$$

We dubbed this technique weighted position loop closure (wPLC). The advantage of wPLC is a better handling of minor movements and especially of periods of standstill which in the naïve equal distribution lead to a generated drift where actually no movement takes place.

Another advantage of the base station is that, for charging, the mower needs to stand in a defined orientation in the base station. We use this property to also apply an orientation loop closure as we know that the start and end orientation of the mower should also be the same. Similar to wPLC we propose to weight the correction of the error. For the orientations we use the absolute rotation as weighting:

$$\theta_{err} = \theta_{end} - \theta_{start} \tag{9}$$

$$\theta_{all} = \sum_i |\Delta\theta_i| \tag{10}$$

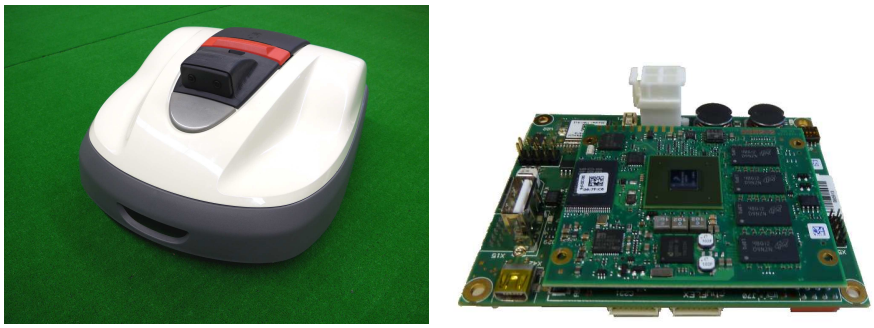
$$\Delta\theta_i^{corr} = \Delta\theta_i - \frac{|\Delta\theta_i|}{\theta_{all}} \theta_{err} \tag{11}$$

We refer to the combined application of weighted orientation and weighted position loop closure as wOPLC. Since the rotation estimation in the differential drive equation (1) is independent of the position estimation, it is favorable for the wheel odometry to first calculate the orientation loop closure and only afterwards calculate the position loop closure.

4 Results

4.1 Hardware Setup

For recording realistic data we use an off-the-shelf autonomous lawn mower and extend it with a stereo camera module that also hosts a mass storage for recording the camera data as well as CAN bus data. Fig. 1 shows the mower with the camera module attached. The module replaces the maintenance lid and thus seamlessly integrates into the lawn mower body. For stereo image capturing and recording we use a phyFLEX-i.MX6 (Fig. 1, right image, top board), with an industrial grade Freescale i.MX6 quad-core processor running Linux OS, manufactured by Phytec Messtechnik GmbH (Mainz, Germany). The reason for the industrial grade is the expected high burden on the electronics due to heat and moisture in the garden environment. Especially, in high summer heat can be a major issue as active cooling is



(a) Test Unit (b) Embedded Board

Fig. 1 (b) Autonomous lawn mower with camera module for image capturing and data recording. (b) Internal embedded board phyFLEX-i.MX6 on top of a base board providing interfaces to the cameras and the mower CAN.

not possible because the cut grass snippets would clog the air intake or the fan after a short time.

For seamless integration of the computing board with the autonomous lawn mower, we use a custom base board (Fig. 1, right image, bottom board also by Phytec) that provides a CAN interface to the phyFLEX-i.MX6 board and that allows a direct connection to the battery power line of the autonomous mower. The overall power consumption of the whole module is 5-7W, and the direct connection to the mower power line allows a fully autonomous operation of our prototype as the mower recharges autonomously without user interaction.

To capture stereo images we use two Phytec camera boards that feature an Aptina MT9V024 automotive CMOS chip with a resolution of 752x480 pixels and global shutter at 20Hz.

4.2 Test Setup

Our primary target is to achieve a good estimation of the outline of the garden shape the autonomous mower is working in. The idea is to let the autonomous mower drive along the boundary wire (in "border cutting mode") and simultaneously record sensor data for estimating the position of movement of the mower. As explained in Section 3, we compare three different methods: wheel odometry, visual odometry and RTK-GPS.

In order to be able to compare the methods, we need representative test gardens and ground truth position data of the boundary wire. To this end, we selected five different gardens in the Frankfurt area that had already an autonomous lawn mower (and accordingly a boundary wire) installed. Fig. 2 shows aerial images of the five selected test gardens. We tried to have test gardens of different size and shape but also of different GNSS occlusion in order to get representative measures for all



(a) Garden 1 (b) Garden 2 (c) Garden 3

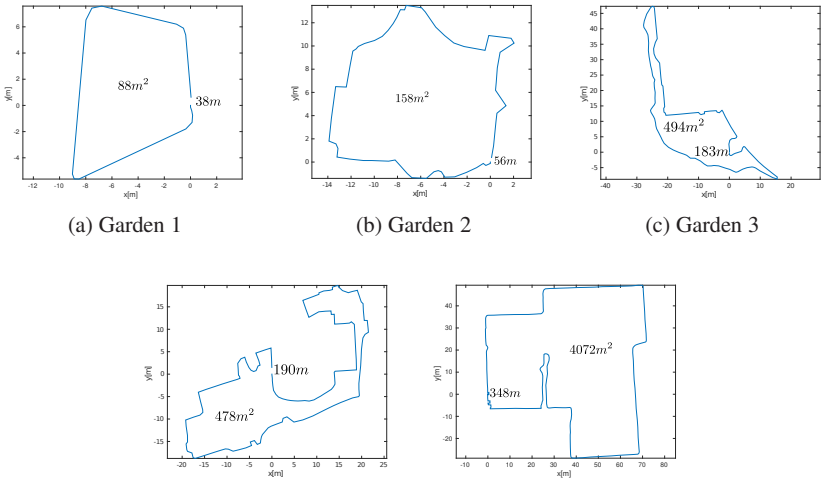
(d) Garden 4 (e) Garden 5

Fig. 2 Aerial images of the five test gardens with the boundary wire layout in white.

methods. Furthermore, by selecting gardens with already installed mower and wire we made sure that the wire was placed without being biased by our experiment.

For ground truth generation of the boundary wire layout we had a land surveyor measure the exact position of the wire. We manually marked between 16 and 183 positions on the wire using pegs. In curves we put more pegs than on the straights in order to get a good approximation of the continuous shape of the wire. The position of the pegs were then accurately measured by the land surveyor with a theodolite. The origin of the local position coordinate system was put in the center of the base station and the orientation of the coordinate system was aligned with the heading of the base station (the direction the mower has to enter for charging). Fig. 3 shows the ground truth layout of all five test gardens as determined by the land surveyor. As can be seen, the size of the gardens varies from $88m^2$ to $4072m^2$ and the shape encompass elongated and roundish structures. The length of the wire ranges from $38m$ in the smallest garden to $348m$ in the largest garden.

The error of the ground truth accuracy is governed by two things. Firstly, it depends on the accuracy of the actual measurement with the theodolite, which is very high ($<$1cm). Secondly, there is an error introduced by placing the pegs. Since in some gardens the wire was buried the placing error is about 3cm as we had to use the mowers internal wire sensor for locating the wire in these cases. Thus, in summary the maximum position error of the ground truth boundary wire layout is 4cm.



(a) Garden 1 (b) Garden 2 (c) Garden 3

(d) Garden 4 (e) Garden 5

Fig. 3 Boundary wire layout in the five test gardens, as determined by the land surveyor.

4.3 Results

In each of the five test gardens we did three types of recordings. Firstly, we recorded wheel rate, yaw sensor and accelerometer data for the wheel odometry. This was done by reading the CAN data from the mower, i.e. we used the internal sensor data of the off-the-shelf mower. The recording rate from the CAN bus was 10Hz. Secondly, we recorded stereo image data for the visual odometry with the Phytec stereo camera. The resolution of the cameras is 752x480 pixels and the images were recorded with 20Hz. Thirdly, we recorded GPS data with the RTK-GPS system, which was just mounted to the top of the autonomous lawn mower. The recording rate was set to 1Hz. Please note that the three types of recording were done in separate runs.

For measuring the accuracy of the different methods we compare the estimated trajectory of the mower driving along the boundary wire to the ground truth data. Although we normalized the ground truth data in position and direction according to the position and direction of the base station, we realized that there are minor differences in orientation of the mower when standing in the base station. These minor orientation differences can amount to gross position differences in the large gardens. To tackle this problem, we apply an Iterative Closest Point algorithm (ICP) [2, 1] for all methods between the estimated trajectory and the ground truth wire layout prior to the error calculation. Note that this has no influence on the goal of our evaluation as we are only interested in the shape of the layout and not its correct global position and orientation.

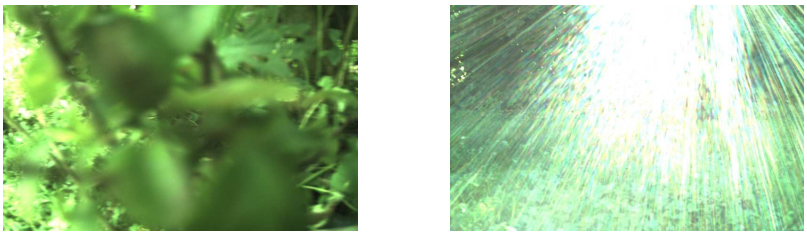
The actual computation of the accuracy is based on point to line distances. Given a trajectory, output by on one of the evaluated methods, we first compute the minimal point to line distance for each trajectory point to the polylines of the ground truth data. We then compute the average minimal point to line distance for all points of the ground truth to the polyline of the trajectory. Finally, we take the maximum of both measures. In the discussion below we will just refer to this measure as average distance.

Table 1 Comparison of visual odometry methods ORB-SLAM and NOTF; plain wheel odometry (WO), yaw sensor enhanced WO with standard loop closure (yWO+LC) and yaw sensor enhanced WO with our proposed weighted orientation and position loop closure (wOPLC); as well as RTK-GPS with altitude information and without. The table entries are average distances between the boundary wire layout estimated by the evaluated methods and the ground truth data. Gardens 1-5 correspond to the gardens seen in Fig. 2 and Fig. 3.

method	garden 1 38m 88m^2	garden 2 56m 158m^2	garden 3 183m 494m^2	garden 4 190m 478m^2	garden 5 348m 4072m^2	avg. error
ORB SLAM	0.26m	0.13m	0.38m	0.91m	1.14m	0.56m
ORB SLAM w/o global BA	0.28m	0.21m	0.33m	2.37m	0.95m	0.83m
NOTF+wPLC	0.22m	0.20m	0.47m	1.46m	1.45m	0.76m
RTK-GPS	0.61m	0.57m	3.90m	1.65m	0.20m	1.39m
RTK-GPS w/o altitude	0.18m	0.33m	0.68m	0.82m	0.24m	0.45m
WO	2.72m	1.38m	4.19m	2.84m	12.57m	4.74m
yWO+LC	0.20m	0.15m	0.76m	0.45m	4.08m	1.13m
yWO + wOPLC	0.19m	0.15m	0.38m	0.24m	0.85m	**0.36m**

The results of the comparison for all evaluated methods (ORB-SLAM, NOTF, WO and RTK-GPS) are summarized in Table 1. For ORB-SLAM we tested two different variants, the original ORB-SLAM and ORB-SLAM with deactivated global bundle adjustment (BA). Since ORB-SLAM is doing a loop closure and a global BA upon loop detection, we analyzed how much the additional BA is contributing.

From the results it can be seen that the additional BA has only a major influence in garden 4. The reason for this is that garden 4 posed a particular difficult setting for the visual odometry. The boundary wire in garden 4 was very close to some bushes, leading to heavy occlusion as the mower drives so close that the camera touches the leaves of the bushes (see Fig. 4a). This of course leads to high estimation errors. As the result in Table 1 shows both NOTF and ORB-SLAM without global BA have a very high error in garden 4. BA significantly reduces the error for ORB-SLAM from 2.37m to 0.91m because the global BA can recover gross misestimations of key frame positions if the surrounding key frames have a good position estimation. Another problem encountered mainly in garden 4 were heavy sun glares (see Fig. 4b). Similar to the occlusions the sun glares lead to wrong feature movements which lead to failure in camera motion estimation.



(a) Occlusion (b) Sun Glare

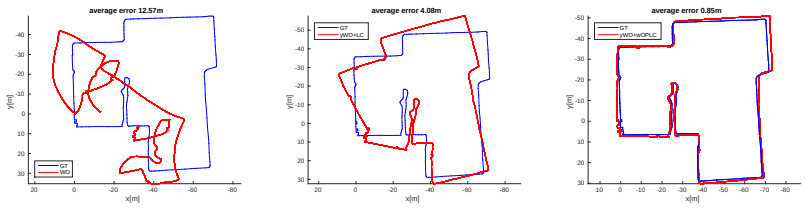
Fig. 4 Encountered issues with the visual odometry. (a) Occlusion in camera view when the mower drives close to a bush in garden 4. (b) Heavy sun glare caused by direct sun.

It is interesting to see that given its simple nature, NOTF is not much worse than ORB SLAM. This means that the internal map building does not yield much more information for the visual odometry than the selection strategy of feature points in NOTF. This is in line with the observations in [4] that even without temporal filtering and map building a high accuracy of VO can be achieved. It should be noted though that we extended the NOTF algorithm with our proposed weighted position loop closure (wPLC) and that the results presented here might not generalize to other application areas where loop detection is not straightforward.

Next we evaluated the RTK-GPS system. The obvious advantage of GPS is that it does not drift with time. However, it is strongly influenced by the 3D layout of the environment. High structures like buildings or trees block the view to some satellites, which reduces the position accuracy. This is directly reflected in the accuracy of the boundary wire layout estimation. Garden 5 has no higher structures which leads to a very high accuracy of 0.2m. Gardens 1 and 2 have only some obstruction while gardens 3 and 4 have many high structures leading to some areas in the garden where position estimation is extremely difficult. Looking at the actual position estimations reveals that the error for RTK-GPS is mainly in the altitude, i.e. the height estimates are very noisy. Thus, we also calculated the average distance for the RTK-GPS with a fixed height (starting height). This leads to a major improvement in almost all gardens.

The last three entries in Table 1 show our results with plain wheel odometry (WO), yaw sensor enhanced WO with standard loop closure (yWO+LC) and yaw sensor enhanced WO with our proposed weighted orientation and position loop closure (yWO+wOPLC). As expected the results with plain WO are not very accurate, mainly due to wheel slip. Using additional yaw sensor data and standard loop closing strongly improves the estimations as the orientation estimation is not influenced by wheel slip anymore. However, in the larger gardens 3-5 the drift of the yaw sensor has a significant impact on the overall accuracy. A visual comparison of the three different WO methods is shown with the resulting maps of garden 5 in Fig. 5.

In the end, we achieved the best overall results with our proposed wOPLC method applied on the yaw sensor enhanced wheel odometry (yWO), which was surprising to us. The evaluation demonstrates that our proposed wOPLC is very

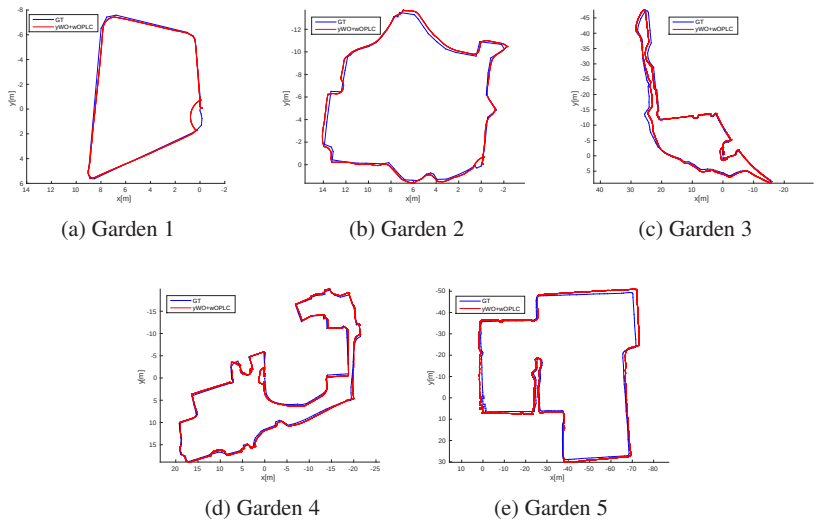


(a) WO (b) yWO+LC (c) yWO+wOPLC

Fig. 5 Comparison of plain wheel odometry (WO), yaw sensor enhanced WO with standard loop closure (yWO+LC) and yaw sensor enhanced WO with our proposed weighted orientation and position loop closure (wOPLC) on the data of garden 5. The blue line is the ground truth layout.

capable of correcting the drift error. Of course the error still increases with driven distance as the higher average layout distance in garden 5 indicates. Nevertheless, it shows that todays autonomous lawn mowers could build a map of the boundary wire with just their internal sensors which opens the way to many functions improving the efficiency and perceived intelligence of the autonomous lawn mowers.

Fig. 6 shows the trajectories estimated by yWO+wOPLC for all test gardens. The plots show the high similarity between the layout estimated by yWO+wOPLC



(a) Garden 1 (b) Garden 2 (c) Garden 3

(d) Garden 4 (e) Garden 5

Fig. 6 Results for our proposed yWO+wOPLC method for all five test gardens overlayed with ground truth (GT) layout measured by the land surveyor.

trajectories and the ground truth boundary wire layout. In all gardens a small arc is visible close to the origin of the coordinate system that deviates from the ground

truth. This is the location of the base station and the arc in the trajectory is caused by the autonomous lawn mower driving around the base station in order to enter it from the correct direction (or to reach the wire after exiting the station).

5 Summary

We presented a comparison of visual odometry (VO), wheel odometry (WO) and RTK-GPS for estimating the layout of the boundary wire of autonomous lawn mower installations. For the evaluation five test gardens were selected and the wire was measured by a land surveyor for ground truth position data.

The result of our comparison shows that WO together with our proposed weighted loop closure shows the best overall results. VO methods struggle with occlusion of the camera when the mower comes very close to objects like bushes, and with heavy sun glare in certain conditions. Furthermore, VO methods would require artificial lighting in night time operation. RTK-GPS also showed good results when only few high structures are located near the garden. Otherwise the accuracy is lower than VO or WO. In particular the altitude is very noisy and not suitable to estimate the slopes in most gardens.

The good performance of WO may be surprising but also means that current off-the-shelf mowers are capable to estimate a boundary wire map with their already equipped internal sensors. Such maps make localization feasible, which in turn opens the way to intelligent functions like automatic start point definition, mowing schedule optimization, direct homing or mowed area bookkeeping.

In the future, we want to investigate the possibility to fuse multiple wire following trajectories in order to improve the accuracy. Also a fusion of the different methods has the potential for canceling out respective weaknesses. In particular, the fusion of the WO with GPS would allow a map with global position data, which in turn would help facilitate the localization of the lawn mower within the garden, especially after a user intervention.

Acknowledgments

We would like to thank Nico Steinhardt for supervising the GNSS prestudy. Furthermore, we want to thank Hideaki Shimamura and Makoto Yamamura for supporting us with the autonomous lawn mower.

References

1. P. J. Besl and N. D. McKay. Method for registration of 3-d shapes. In *Robotics-DL tentative*, pages 586–606, 1992.
2. Y. Chen and G. Medioni. Object modelling by registration of multiple range images. *Image and vision computing*, 10(3):145–155, 1992.
3. H. Şahin and L. Güvenç. Household robotics: Autonomous devices for vacuuming and lawn mowing. *IEEE Control Systems*, 27(2):20–96, 2007.
4. J. Deigmöller and J. Eggert. Stereo visual odometry without temporal filtering. In *German Conference on Pattern Recognition (GCPR)*, pages 166–175, 2016.
5. G. Dudek and M. Jenkin. *Computational principles of mobile robotics*. Cambridge university press, 2010.
6. J. Fink, V. Bauwens, F. Kaplan, and P. Dillenbourg. Living with a vacuum cleaning robot. *International Journal of Social Robotics*, 5(3):389–408, 2013.
7. A. Geiger, P. Lenz, and R. Urtasun. Are we ready for autonomous driving? the KITTI vision benchmark suite. In *IEEE Conference on Computer Vision and Pattern Recognition (CVPR)*, pages 3354–3361, 2012.
8. M. Hägele, editor. *World Robotics 2016 Service Robots*. International Federation of Robotics Statistical Department, 2016.
9. R. W. Hicks and E. L. Hall. Survey of robot lawn mowers. In *Intelligent Robots and Computer Vision XIX: Algorithms, Techniques, and Active Vision*, 2000.
10. M.-J. Jung, H. Myung, S.-G. Hong, D.-R. Park, H.-K. Lee, and S. Bang. Structured light 2D range finder for simultaneous localization and map-building (SLAM) in home environments. In *Micro-Nanomechatronics and Human Science, and The Fourth Symposium Micro-Nanomechatronics for Information-Based Society*, pages 371–376, 2004.
11. H.-K. Lee, K. Choi, J. Park, and H. Myung. Self-calibration of gyro using monocular SLAM for an indoor mobile robot. *International Journal of Control, Automation and Systems*, 10(3):558–566, 2012.
12. S. Lee, S. Lee, and S. Baek. Vision-based kidnap recovery with SLAM for home cleaning robots. *Journal of Intelligent & Robotic Systems*, 67(1):7–24, 2012.
13. A. Levratti, C. Secchi, and C. Fantuzzi. A low cost localization algorithm for an autonomous lawnmower. In *Robot Motion and Control (RoMoCo), 2013 9th Workshop on*, pages 276–281. IEEE, 2013.
14. B. Metka, A. Besetzny, U. Bauer-Wersing, and M. Franzius. Predicting the long-term robustness of visual features. In *International Conference on Advanced Robotics (ICAR)*, pages 465–470. IEEE, 2015.
15. R. Mur-Artal and J. D. Tardos. ORB-SLAM2: an open-source SLAM system for monocular, stereo and RGB-D cameras. *arXiv preprint arXiv:1610.06475*, 2016.
16. E. Prassler, M. E. Munich, P. Pirjanian, and K. Kosuge. Domestic robotics. In *Springer Handbook of Robotics*, pages 1729–1758. 2016.
17. T. Stone, D. Differt, M. Milford, and B. Webb. Skyline-based localisation for aggressively manoeuvring robots using UV sensors and spherical harmonics. In *IEEE International Conference on Robotics and Automation (ICRA)*, pages 5615–5622. IEEE, 2016.
18. S. Thrun, D. Fox, W. Burgard, and F. Dellaert. Robust monte carlo localization for mobile robots. *Artificial Intelligence*, 128(1–2):99–141, 2001.
19. C. Valgren and A. J. Lilienthal. SIFT, SURF & seasons: Appearance-based long-term localization in outdoor environments. *Robotics and Autonomous Systems*, 58(2):149–156, 2010.
20. J. Yang, S.-J. Chung, S. Hutchinson, D. Johnson, and M. Kise. Vision-based localization and mapping for an autonomous mower. In *IEEE/RSJ International Conference on Intelligent Robots and Systems (IROS)*, pages 3655–3662, 2013.
21. J. Yang, S.-J. Chung, S. Hutchinson, D. Johnson, and M. Kise. Omnidirectional-vision-based estimation for containment detection of a robotic mower. In *IEEE International Conference on Robotics and Automation (ICRA)*, pages 6344–6351, 2015.